



ELSEVIER

Thin Solid Films 388 (2001) 73–77



www.elsevier.com/locate/tsf

# Synthesis of well-aligned multiwalled carbon nanotubes on Ni catalyst using radio frequency plasma-enhanced chemical vapor deposition

G.W. Ho<sup>a</sup>, A.T.S. Wee<sup>a</sup>, J. Lin<sup>a,\*</sup>, W.C. Tjiu<sup>b</sup>

<sup>a</sup>*Department of Physics, Surface Science Laboratory, National University of Singapore, 10 Kent Ridge Crescent, Singapore 119260, Singapore*

<sup>b</sup>*Institute of Materials Research and Engineering, 3 Research Link, Singapore 1176020, Singapore*

Received 18 April 2000; received in revised form 23 January 2001; accepted 23 January 2001

## Abstract

Well-aligned multiwalled nanotubes (MWNTs) have been deposited by plasma-enhanced chemical vapor deposition of acetylene ( $C_2H_2$ ) on nickel-coated quartz glass at  $650^\circ C$ . The growth reaction of the carbon nanotubes was found to be dependent on the morphology of the metal catalyst, which was related to the thickness of the Ni catalyst film. The flow rate of the hydrocarbon gases was observed to be crucial for the growth of high density carbon nanotubes. Well-aligned and dense carbon nanotubes were grown uniformly on 15-nm thick Ni film with a flow rate of 15 and 30 sccm for  $C_2H_2$  and  $NH_3$ , respectively. Transmission electron microscopy confirmed the structures to be hollow with Ni particles encapsulated by the multi-walls at the tip of the nanotube. © 2001 Elsevier Science B.V. All rights reserved.

**Keywords:** Carbon nanotubes; Graphite; Nickel; Chemical vapor deposition

## 1. Introduction

The discovery of carbon nanotubes [1] has caused tremendous excitement as it has opened up a new field of carbon chemistry. A carbon nanotube is a honeycomb lattice with large individual graphene layers where the buckyball structure is extended to form long slender tubes. Carbon nanotubes can be grown by arc discharge of carbon electrodes and catalytic methods. Plasma enhanced hot filament chemical vapor deposition (PE-HF-CVD) has been used to grow large arrays of well-aligned carbon nanotubes [2,3]. The catalytic growth of carbon nanotubes is made possible via the decomposition of hydrocarbons (acetylene, methane, benzene, etc.). The growth of carbon nanotubes is

promoted by the precipitation from transition metals of sub-micron diameters. Intensive investigation has been carried out by researchers to elucidate its growth mechanisms [4–7], structural and electronic properties [8,9], as well as potential applications [10,11]. Owing to its unique properties, carbon nanotubes attract much interest as constituents of novel nanoscale materials and devices [12,13]. Researchers are focusing on carbon nanotubes for possible uses ranging from tips for scanning probe microscopes, electron guns for flat panel displays to storage of gases [11]. In our work, we studied carbon nanotubes grown by plasma-enhanced decomposition of a mixture of ammonia and acetylene gases on a Ni catalyst film.

## 2. Experimental

The synthesis of carbon nanotubes was carried out by the decomposition of acetylene and ammonia gases

\* Corresponding author. Tel.: +65-874-2616; fax: +65-874-6126.  
E-mail address: phylin@nus.edu.sg (J. Lin).

on Ni thin-films in a modified Plasma Quest series III PQM-9157-A, plasma-enhanced chemical vapor deposition (PECVD) chamber. The base pressure of the chamber was  $5 \times 10^{-6}$  torr. Thin Ni films of various thicknesses on quartz glass were prepared by radio frequency magnetron sputtering at room temperature, with different sputtering times of 45, 150 and 210 min. The thicknesses of the films grown were 10, 15 and 25 nm, respectively. The effect of gas flow rate was investigated by varying the flow rate of reactive gases. Carbon nanotubes were grown at 1000 mtorr with 90 W RF power. After the working pressure was stabilized, a heating core cable powered by an AC source was used to generate heat. The synthesis temperature for the carbon nanotube growth was estimated to be  $650^\circ\text{C}$  as measured by a thermocouple. The growth time of the carbon nanotubes was kept constant at 30 min.

A field emission scanning electron microscope (FESEM), JSM JEOL 6430F was used to study the density, alignment, tube diameter and length of the carbon nanotubes at 3 kV. The surface topography of the films was imaged by a Digital Instruments Nanoscope multimode TM D3000 series atomic force microscope (AFM) in tapping mode. Structural information was obtained using a high-resolution transmission electron microscope (HRTEM) Philips CM300 FEG at 300 kV. Carbon nanotubes grown on the Ni films were dispersed by an ultrasonic bath of acetone and transferred onto a copper TEM grid lined with formvar support film. Raman scattering study was performed using a SPEX 1702/04 Spectrometer equipped with an Olympus BH2-um4 optical microscope, which allows measurements of Raman spectra with a spatial resolution of  $0.7 \mu\text{m}$ . Samples were excited by an  $\text{Ar}^+$  laser at a wavelength of  $\lambda = 488 \text{ nm}$ . The acquisition time for the spectra was 60 s with no smoothing applied to the spectra. Measurements were carried out at room temperature.

### 3. Results and discussion

Fig. 1a shows a SEM image of vertically aligned carbon nanotubes grown on 15-nm thick Ni film [written as Ni (15 nm) film]. The flow rate of the  $\text{C}_2\text{H}_2$  and  $\text{NH}_3$  used was 15 and 30 sccm, respectively. Part of the carbon nanotube array was peeled off by tweezers to analyse the orientation and physical properties of the tubes. A striking feature of the as-grown carbon nanotubes on Ni (15-nm) film is the uniform length of high density nanotubes. The alignment of the nanotubes across the whole surface is uniform. The tubes are  $50\text{--}100 \text{ nm}$  in diameter and  $8\text{--}9 \mu\text{m}$  in length. The rate of growth was  $17 \mu\text{m/h}$ . The high magnification SEM image in Fig. 1b shows that Ni particles appear to cap each tube. This is further confirmed using energy dispersive X-ray (EDX) analysis which shows a strong Ni

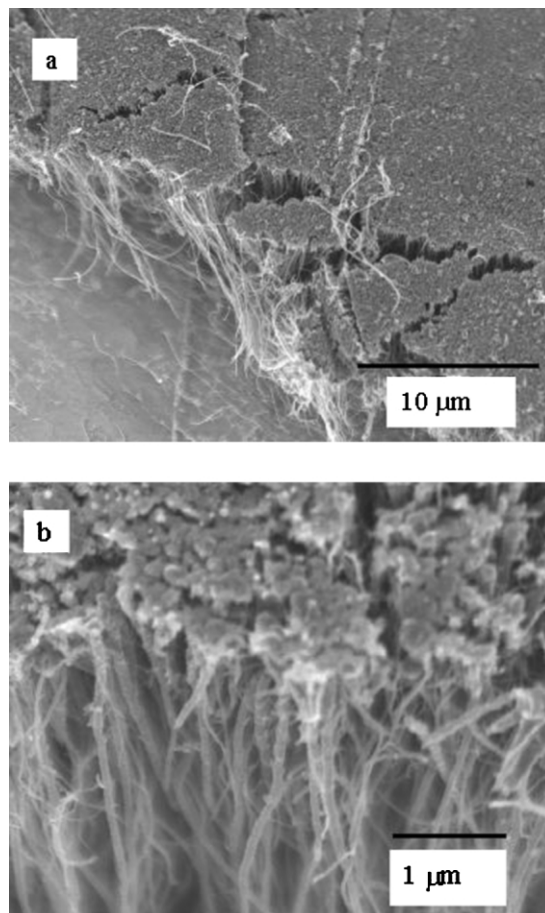


Fig. 1. SEM micrographs of carbon nanotube grown on (a) Ni (15 nm) film and (b) Ni (15 nm) film (high magnification).

signal in addition to C. In contrast, dense and vertically aligned nanotubes are found only on scattered islands of Ni (10 nm) and Ni (25 nm) films as thick ( $\sim 200 \text{ nm}$ ), short ( $\sim 1 \mu\text{m}$ ), but sparse carbon nanotubes.

When the flow rate of  $\text{C}_2\text{H}_2$  and  $\text{NH}_3$  was decreased by 3 times, to 5 and 10 sccm, respectively, sparse carbon nanotubes, which co-exist with graphite particles, were found on all the samples. SEM results show that only a few relatively short ( $\sim 2 \mu\text{m}$ ) nanotubes grown on Ni (15 nm) film are vertically aligned as most of the long nanotubes ( $\sim 10 \mu\text{m}$ ) lie parallel to the surface. Both Ni (10 nm) and Ni (25 nm) films produced randomly oriented and not vertically aligned nanotubes. Generally, Ni particles were not observed at the tip of the tubes for all the three samples grown at relatively lower flow rates of the gases. The diameters of the outer dimension of the nanotubes were in the same range as the Ni particles. This suggests that the morphology of the Ni film affects the growth of the carbon nanotubes.

Surface morphology and related thickness values of the deposited Ni catalyst films are summarized in Table 1. Particular attention has been given to factors such as

Table 1  
Morphology of Ni film at various deposition times

Deposition time/min	Thickness/nm	Roughness/nm (rms)	Grain size/nm	Density/ $\mu\text{m}^2$
45	10	2.8	50–90	25
150	15	3.4	50–200	10
210	25	1.1	Not defined	Not defined

roughness, grain size and density, which ultimately affect the growth of the carbon nanotubes. The SEM image Ni (10 nm) in Fig. 2a shows randomly oriented Ni grains of 50–90 nm in diameter with relative regular round shapes. This SEM image shows that the film is in the island growth stage typical of early film deposition. The islands contain denser Ni crystallites. AFM rms roughness is 2.8 nm and the density of the Ni grains is  $25/\mu\text{m}^2$ . As the deposition time increased to 150 min, Ni (15 nm) of Fig. 2b exhibits a larger grain size distribution of  $\sim 50$ –200 nm. AFM rms roughness is 3.4 nm and the density of the Ni grains is  $10/\mu\text{m}^2$ . The islands acting as nucleation centers grew in size by coalescence resulting in the formation of elongated grains. Furthermore, increase in deposition time to 210 min resulted in a thick Ni film shown in Fig. 2c. Coalescence of Ni grains proceeded until the film was almost continuous, which involved filling up of voids between the large islands. This results in a smoother surface Ni film as indicated by the AFM rms roughness measurement of 1.1 nm. There are no well-defined grain boundaries as the Ni film becomes more uniform.

Among the experimental conditions tried, the best vertically aligned carbon nanotubes were obtained on Ni (15 nm) films when the flow rates of  $\text{C}_2\text{H}_2$  and  $\text{NH}_3$  gases were 15 and 30 sccm, respectively. It is believed that the 15-nm thick Ni film promotes carbon nanotube nucleation since it comprises Ni particles 50–200 nm in diameter, which have comparable dimensions to the nanotube diameters. AFM surface roughness measurements show that the Ni (15-nm) film is rougher than the other samples. It is postulated that rougher surfaces, associated with larger surface areas provide an increased number of sites for carbon nanotube growth. It is possible to deduce that a higher flow rate of gases has a significant impact on the density of carbon nanotubes. Sufficient supply of carbon atoms from the hydrocarbon source allows the formation of dense nanotubes, which ultimately forces the nanotubes to align vertically due to steric hindrance from neighboring tubes [14]. This can be seen on the Ni (15-nm) film in Fig. 1 where the alignment of the nanotubes across the whole surface is uniform and dense.

Changes to the gas flow rates have no effect on the Ni (25 nm) film as sparse and thick (100–150-nm di-

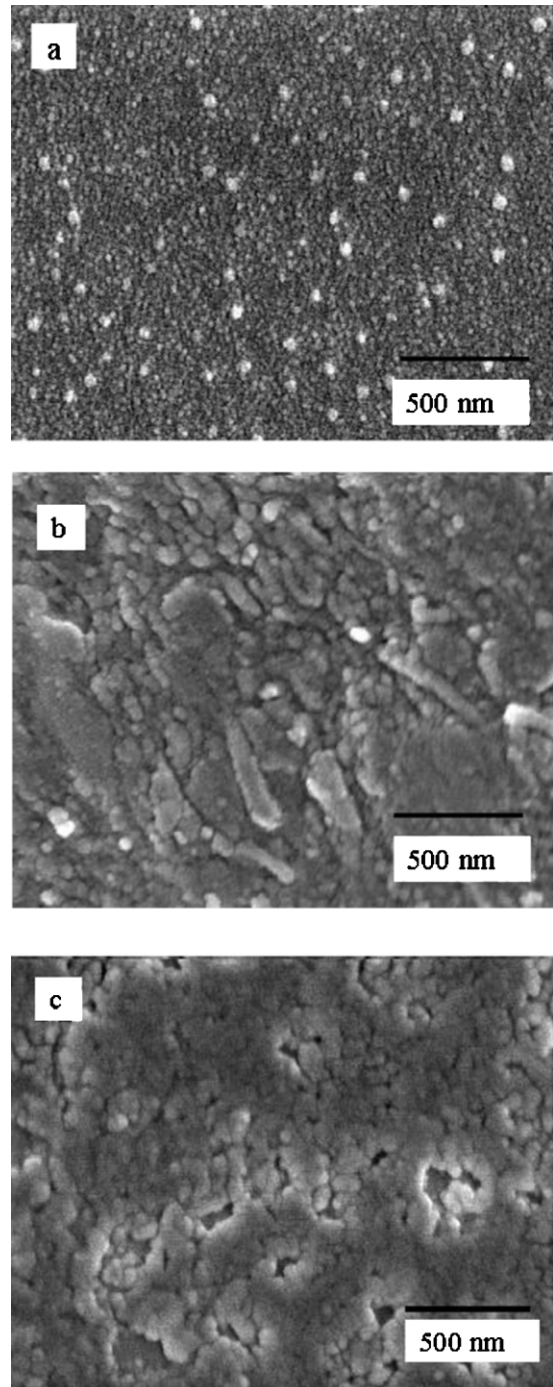


Fig. 2. SEM micrographs of Ni films deposited for (a) 45 min Ni (10 nm), (b) 150 min Ni (15 nm) and (c) 210 min Ni (25 nm).

ameter) nanotubes with graphite particles were observed. This may be explained by the absence of well-defined grains on the quartz glass, which inhibits nanotube formation. This is in agreement with Yudasaka et al. [15] who proposed that graphite sheets generated by CVD that initially cover the Ni particles will transform into carbon nanotubes only when there is a presence of nanometer-sized Ni particles since the mechanical stress of the graphite will exceed the elastic limit required for the transformation to take place. It is also noted that Ni particles on the thin Ni (10-nm) film are unfavorable for the growth of dense and vertically aligned carbon nanotubes as the Ni crystallites comprising small islands are sparse and scattered. Thus, the growth kinetics of well-aligned carbon nanotubes is governed by the morphology of the Ni film and the flow rate of the gases.

Fig. 3 shows a high resolution TEM image of a typical carbon nanotube grown at flow rates of 15 sccm  $C_2H_2$  and 30 sccm  $NH_3$ . It confirms the presence of hollow nanotubes rather than solid nanofibers. We observe multi-layered carbon nanotubes along with graphite particles. It is believed that the growth mechanism is very similar to the work done by Yudasaka et al. [16] where graphite layers generated by CVD on Ni particles of optimum diameter transform into nanotubes enclosing the Ni particles under specific conditions. During carbon nanotube growth, the Ni particle at the carbon nanotube tip plays the role of an active catalyst. When the temperature is sufficiently lowered after the growth process, the nanotube may close with the formation of curvature-induced defects thus encapsulating the Ni catalyst particle.

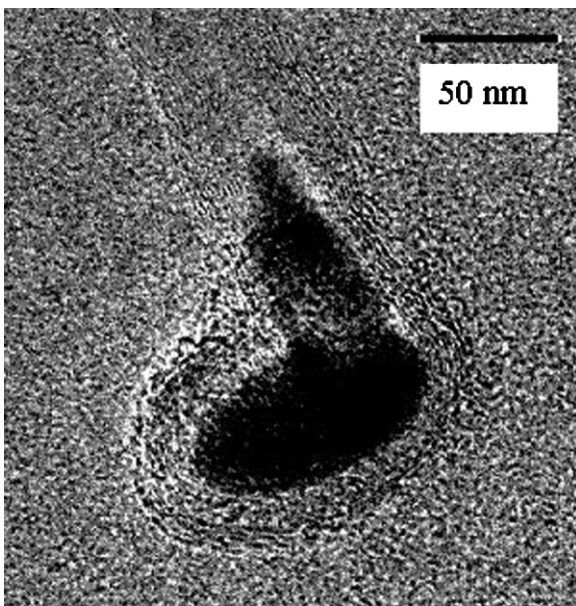


Fig. 3. TEM image of a typical carbon nanotube encapsulating a nickel particle.

ulating the Ni catalyst particle. The Ni catalyst particle can measure between 50 and 200 nm in diameter. The closure prevents dangling bonds with very little strain thus minimizing the energy. There are usually six or more graphene layers in the carbon nanotube walls. Visible defects are observed along the growth direction of carbon nanotubes grown at a relatively lower temperature of 650°C because well-graphitized carbon nanotubes are produced only at higher temperatures.

Raman spectroscopy was used to confirm the composition of carbon nanotubes and graphite particles. No graphite peaks were observed in the spectrum before the PECVD process. The Raman spectrum of the scattered growth of carbon nanotubes on Ni (10 nm) film is ascribed to amorphous carbon, apparent from the broad peaks of disordered graphite approximately 1583 and 1358  $cm^{-1}$ . Similarly, broad graphite peaks are observed on the Ni (15-nm) film grown at relative low flow rate of gases. Both peaks are characteristic of graphite. The 1358  $cm^{-1}$  is the  $A_{1g}$  lattice vibration mode and the additional line at 1583  $cm^{-1}$  is the G line, the high frequency  $E_{2g}$  first-order mode [17]. As the thickness of the Ni film increases to 25 nm, the Raman spectrum becomes more characteristic of graphite as the peaks become relatively sharper. It was also observed that the Raman spectra of the well-aligned dense carbon nanotubes of Ni (15-nm) film grown at higher gas flow rates shifts to 1577  $cm^{-1}$ . This shift may indicate the presence of higher purity carbon nanotubes as it is expected that the bending of graphite layers into a nanotube cylinder should shift the graphite line to 1575  $cm^{-1}$  [18].

The growth mechanism in our work is catalyst-based where Ni promotes graphite formation. It is known that Ni promotes graphite formation through the dehydrogenation process [19]. Metal catalytic growth of the carbon nanotube is postulated to occur via solvation of carbon vapor into the metal cluster on the substrate. A carbon-metal alloy promotes diffusion of carbon into the metal alloy and allows the nucleation of carbon and subsequently, formation of nanotubes. The physical mechanisms of catalytic grown carbon nanotubes may be tip or base growth [20]. SEM images have provided some insights into the growth mechanisms. It is noted that carbon nanotubes grown at lower gas flow rates produced carbon nanotubes with mostly catalyst-free tube ends as most Ni particles strongly adhere to the substrate, resulting in base growth [20]. On the other hand, high gas flow rates produced nanotubes with residual metallic catalysts at the tip of the tube. This may suggest that high gas flow rates weaken the contact force between the catalyst and substrate resulting in tip growth [21]. It is postulated that tip growth causes nanotubes of uniform height, as the carbon atom supply does not have to diffuse to the base and is uniform at the tips of the nanotubes.

#### 4. Conclusion

We have successfully synthesized dense and well-aligned MWNTs using plasma-enhanced chemical vapor deposition at relatively low temperatures. The growth of carbon nanotubes on the 15-nm thick Ni film is the most favorable among the three different thicknesses studied. Large areas of uniform and well-aligned carbon nanotubes require Ni particles of approximate density of  $\sim 10/\mu\text{m}^2$  and diameter of  $\sim 50\text{--}200$  nm. The tubes are found to align vertically when high density carbon nanotubes growth is observed. The growth and alignment of the carbon nanotubes was found to be strongly-dependent on the morphology of metal catalyst as well as the flow rate of gases.

#### Acknowledgements

The authors would like to thank Mr G.S. Chen for his assistance in the operation of plasma-enhanced chemical vapor deposition and Dr Z.X. Shen for the use of Raman Spectrometer.

#### References

- [1] S. Iijima, *Nature* 354 (1991) 56.
- [2] Z.F. Ren, Z.P. Huang, J.W. Xu, J.H. Wang, P. Bush, M.P. Siegal, P.N. Provencio, *Science* 282 (1998) 1105.
- [3] Z.P. Huang, J.W. Xu, Z.F. Ren, J.H. Wang, M.P. Siegal, P.N. Provencio, *Appl. Phys. Lett.* 73 (1998) 3845.
- [4] T.W. Ebbesen, *Carbon Nanotubes Preparation and Properties*, Chemical Rubber, Boca Raton, 1997.
- [5] J.C. Charlier, A.De Vita, X. Blasé, R. Car, *Science* 275 (1997) 646.
- [6] S.H. Tsai, C.W. Chao, C.L. Lee, H.C. Shih, *Appl. Phys. Lett.* 74 (1999) 3462.
- [7] W.Z. Li, S.S. Xie, L.X. Qian, B.H. Chang, B.S. Zou, W.Y. Zhou, R.A. Zhao, G. Wang, *Science* 274 (1996) 1701.
- [8] R.A. Jinshi, J. Bragin, L. Lou, *Phys. Rev. B* 59 (1999) 9862.
- [9] C.T. White, D.H. Robertson, J.W. Mintmire, *Phys. Rev. B* 47 (1993) 5485.
- [10] A.C. Dillon, K.M. Jones, T.A. Bekkedahl, C.H. Kiang, D.S. Bethune, M.J. Heben, *Nature* 386 (1997) 377.
- [11] P. Chen, X. Wu, J. Lin, K.L. Tan, *Science* 285 (1999) 91.
- [12] W.A. de Heer, A. Chatelain, D. Ugarte, *Science* 270 (1995) 1179.
- [13] C. Niu, E.K. Sichel, R. Hoch, D. Moy, H. Tenent, *Appl. Phys. Lett.* 70 (1997) 1480.
- [14] J.L. Cheol, W.K. Dae, J.L. Tae, C.C. Young, S.P. Young, H.L. Young, B.C. Won, S.L. Nae, P. Gyeong-Su, M.K. Jong, *Chem. Phys. Lett.* 312 (1999) 461.
- [15] M. Yudasaka, R. Kikuchi, Y. Ohki, E. Ota, S. Yoshimura, *Appl. Phys. Lett.* 70 (1997) 1817.
- [16] M. Yudasaka, R. Kikuchi, T. Matsui, Y. Ohki, E. Ota, S. Yoshimura, *Appl. Phys. Lett.* 67 (1995) 2477.
- [17] T.C. Chieu, M.S. Dresselhaus, M. Endo, *Phys. Rev. B* 26 (1982) 10530.
- [18] W.S. Bacsá, D. Ugarte, A. Chatelain, W.A. de Heer, *Phys. Rev. B* 50 (1994) 15473.
- [19] M. Yudasaka, R. Kikuchi, T. Matsui, K. Tasaka, Y. Ohki, S. Yoshimura, E. Ota, *J. Vac. Sci. Technol. A* 13 (1995) 2142.
- [20] G. Che, B.B. Lakshmi, R.E. Fisher, C.R. Martin, *Nature* 393 (1998) 346.
- [21] Y. Gao, J. Liu, M. Shi, S.H. Elder, J.W. Virden, *Appl. Phys. Lett.* 74 (1999) 3642.